

Study of the interaction between glucosamine hydrochloride and sodium dodecylsulphate micelles using conductometric, isothermal calorimetry, zeta-potential titrations, and NMR NOESY

Marcos Roberto Abreu ALVES¹, Luciano Sindra VIRTUOSO²,
Elson Santiago de ALVARENGA³, Ângelo Márcio Leite DENADAI^{4,*}

¹Department of Materials Engineering, Federal University of Itajubá (UNIFEI), Itabira-MG, Brazil

²Department of Chemistry, Federal University of Alfenas (UNIFAL), Alfenas-MG, Brazil

³Department of Chemistry, Federal University of Viçosa (UFV), Viçosa-MG, Brazil

⁴Pharmaceutical Department, Federal University of Juiz de Fora (UFJF), Campus Governador Valadares, Governador Valadares-MG, Brazil

Received: 12.06.2013 • Accepted: 28.08.2013 • Published Online: 14.03.2014 • Printed: 11.04.2014

Abstract: The aim of this work was to investigate the influence of an anti-inflammatory agent, the bulky counterion named glucosamine (Gl^+), in sodium dodecylsulphate (SDS) in 2 ways: 1) by titration of SDS solutions with different concentrations of Gl^+ ; and 2) by titration of Gl^+ with SDS solution with concentration close to the critical micellar concentration (cmc) (7.7 mM). In procedure 1, micellisation study by isothermal titration calorimetry (ITC) showed that the increase in Gl^+ concentration reduces the cmc and the micellisation enthalpy. Increasing of the micellisation entropy was also observed, suggesting desolvation of micellar structures as a consequence of electrostatic attraction with Gl^+ ions. In procedure 2, titration of Gl^+ with SDS solution at 7.7 mM showed the existence of 3 distinct ranges of glucosamine/SDS concentrations, which were attributed to I) Gl^+ inducing micellisation, II) neutralisation of the micelles, and III) competition between the ions themselves in the micellar surface.

Key words: SDS, micelles, glucosamine hydrochloride, osteoarthritis

1. Introduction

The binding of water-soluble molecules such as drugs, antibodies, and antimicrobials to membrane models is an important issue in many biological processes, since it helps us to understand their local mechanism of action.^{1–6} Independent of the target, the initial interaction with cells should occur through contact with the membrane. Thus, there are, for instance, several kinds of cationic substances that bind to the bacterial membrane through electrostatic interactions with negatively charged phospholipids in the outer leaflet of the lipid bi-layer, causing inactivation of ionic channels.

Surfactants are an important kind of substance that are used in many biological, pharmaceutical, and industrial systems, and they tend to self-associate, forming structures such as micelles, vesicles, bi-layers, and bi-continuous systems.^{2,4,5,7–10} Generally their hydrophobic portion is protected from the aqueous environment by an approximately spherical shell formed by the polar or ionic head groups. Thus, the surfactants are able of reducing the liquid–liquid, liquid–solid, and liquid–gas interfacial tension and promote the dissolution of hydrophobic substances such as drugs, dyes, polymers, and oils.

*Correspondence: angelo.denadai@ufjf.edu.br

Micelles of surfactants, such as SDS, are able to induce changes in the secondary structure of peptides and proteins, in addition to interacting strongly with cationic substances. Thus, they have been used as a model of membranes to simulate binding studies of proteins, peptides, and drugs due to some similarities with anionic biological membranes.^{3,11–15}

Glucosamine hydrochloride (Gl^+) (Figure 1) is an anti-inflammatory agent having an excellent toxicity profile,^{16–18} and is an active drug needed to form collagen, whose oral ingestion causes reduction of osteoarthritis.^{16,18–21} Its mode of action is reported to occur in the intracellular environment. It fully protects the chondrocytes from IL-1-induced expression of inflammatory cytokines, chemokines, and growth factors as well as proteins involved in prostaglandin E-2 and nitric oxide synthesis. It also blocks the IL-1-induced expression of matrix-specific proteases such as MMP-3, MMP-9, MMP-10, MMP-12, and ADAMTS-1.²⁰ Although Gl^+ is currently used in therapies, with known action occurring in the intracellular environment, its mechanism of absorption is not yet fully known.

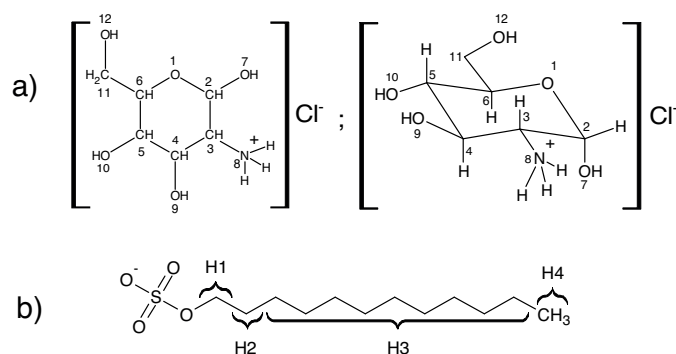


Figure 1. a) Structure of glucosamine hydrochloride and b) SDS.

Our hypothesis is based on the fact that Gl^+ is a hydrophilic species that could interact with anionic cytoplasmic membranes by electrostatic interactions. Moreover, its bulky volume will hinder the crossing of the hydrophobic inner of membranes, increasing the tendency of accumulation in the extracellular environment. Thus, the main objective of this work was to investigate the association between Gl^+ cation with anionic SDS micelles as a membrane model in aqueous solution, since that could represent a contribution for understanding the mechanism of interaction.

Initially, our strategy was based on investigation of the Gl^+ concentration effect on the critical micellar concentration (cmc) of SDS as well as on the thermodynamic properties of micellisation by isothermal titration calorimetry (ITC), once enthalpy and entropy obtained by ITC studies are highly dependent from electrostatic interactions as well as solvation/desolvation balance. Furthermore, we investigated the effect of increasing Gl^+ concentration on SDS solution at 7.7 mM (close to $\text{cmc} = 8.1$ mM), monitored by conductometric, calorimetric, and zeta potential (ZP) titrations. Finally, we investigated the topology of Gl^+ /SDS assembly by NMR NOESY, which allowed us to infer about the depth of Gl^+ in SDS micelles.

2. Experimental section

2.1. Chemicals

The surfactant sodium dodecyl sulphate (SDS) used in the present work was purchased from Merck (purity, 99.9%), and showed a $\text{cmc} = 8.1$ mM, by conductometric titration at 25 ± 0.1 °C. The glucosamine hydrochloride

ride was obtained from Sigma (purity, 99.9%). All the solutions were prepared in purified water (Milli-Q, conductivity 1.22 $\mu\text{S}/\text{cm}$) obtained from a Millipore water purification unit.

2.2. Methods

2.2.1. Isothermal titration calorimetry

The isothermal titration calorimetry (ITC) was carried out using a Microcal VP-ITC Microcalorimeter, at 298 K (25.0 ± 0.1 °C supplied by Peltier thermoelectric system). Titrations were performed in 2 ways: 1) by 51 successive injections of SDS solution at 105.0 mM in a calorimetric cell containing 1.5 mL of Gl^+ solutions at concentrations of 0, 1.0, 3.0, 5.0, 7.0, 10.0, and 15.0 mM; and 2) through of 51 successive injections of Gl^+ aqueous solution (5.0 μL , 65.0 mM) into the reaction cell charged with 1.5 mL of SDS aqueous solution at 7.7 mM. In all experiments, the injections were performed at time intervals of 300 s and stirring speed of 150 rpm. The initial 1.0- μL injection was discarded in order to eliminate diffusion effects from the syringe tip during the pre-equilibration process. The concentration correction as well as the integration of the heat flow peaks to calculate partial molar enthalpy of SDS ($dQ/d[\text{SDS}] = \Delta_{\text{SDS}}H^0$) or the partial molar enthalpy of Gl^+ ($dQ/d[\text{Gl}^+] = \Delta_{\text{Gl}}H^0$) was performed with the software Microcal Origin 5.0 for ITC.

2.2.2. Conductometric titrations

Conductivity measurements were carried out at 298 K (25.0 ± 0.2 °C) with a Tecnal Tec-4MP conductivimeter, through the manual injection of consecutive aliquots of 100 μL of Gl^+ 50.0 mM into a cell charged with 25.0 mL of SDS 7.7 mM upon magnetic stirring. The temperature was controlled by immersion of the cell into a Tecnal TE-184 thermostatic bath.

2.2.3. Zeta potential

ZP measurements were obtained with a Malvern Zetasizer NanoZS with a 64-channel correlator and 633 nm red laser. The technique used for ZP measurement is the Malvern standard laser Doppler velocimetry coupled with M3-PALS (phase analysis light scattering). The sample cell used was the Malvern Folded Capillary cell (DTS1060) of polyethylene with 1 cm of optical length and coupled with electrodes. The experiment proceeded by titration with 51 manual injections of 10.0 μL of the Gl^+ (65.0 mM) into the beaker with 3.0 mL of SDS solution (7.7 mM). After each titration, the solution was transferred to a folded capillary cell and the measurement carried out at 298 K. Each point of ZP corresponds to the average of 5 measurements of 10 runs each.

2.2.4. NMR NOESY experiments

NMR NOESY experiments were carried out on a Varian Mercury spectrometer at a proton resonance frequency of 300 MHz at 298 K (25.0 ± 0.2 °C). All experiments were done with 160 scans, 64 transients, 2 s relaxation delay, 1981 Hz spectral width, and 0.4 s mixing time. In the t₂- and t₁-dimension the free induction decays (FIDs) were apodised with a shifted gaussian window function prior to the Fourier transformation. The solution used in NMR NOESY was SDS (15 mM)/ Gl^+ (5 mM) in D₂O obtained from Sigma-Aldrich, with isotopic purity of deuterium >99.8%.

3. Results and discussion

3.1. SDS micellisation study at different Gl^+ concentrations

Initially, the interaction between SDS and Gl^+ was studied by evaluation of the effect of the Gl^+ cation on the thermodynamic parameters of micellisation: cmc, enthalpy ($\Delta_{mic}H^0$), entropy ($T\Delta_{mic}S^0$), and free energy ($\Delta_{mic}G^0$). Experiments were accomplished by measurement of enthalpy changes associated with titration of micellar surfactant aqueous solution (105.0 mM) with different Gl^+ aqueous solutions at 3.0, 5.0, 10.0, and 15.0 mM, at 298.15 K.

Figure 2 presents ITC experiments in terms of the enthalpy change per injection ($\Delta_{inj}H^0$) as a function of surfactant concentration. As can be observed, each curve exhibits an inflexion point, which was attributed to the cmc. Moreover, the demicellisation enthalpy was calculated by the difference between the enthalpy value on cmc, $[\Delta_{inj}H^0]_{cmc}$, from the first injection value $[\Delta_{inj}H^0]_0$, obtained in each experiment through Eq. (1):

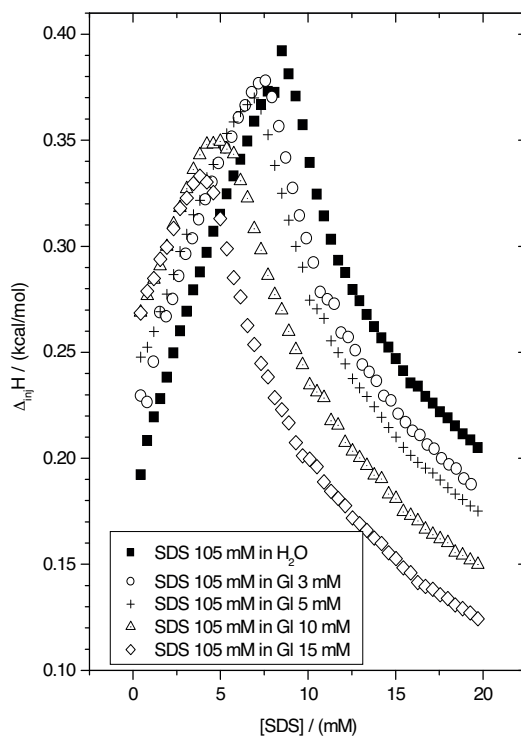


Figure 2. ITC data for titration of SDS 105 mM into cell charged with different concentrations of Gl^+ (0, 3.0, 5.0, 10.0, and 15 mM), in water (pH 6.9) at 298.15 K.

$$\Delta_{dem}H^0 = \left(\frac{\partial \Delta_{inj}H^0}{\partial [SDS]} \right)_{cmc} - \left(\frac{\partial \Delta_{inj}H^0}{\partial [SDS]} \right)_0 \quad (1)$$

Before the cmc, the enthalpy corresponds to the solvation heat of monomers upon breakdown of micelles, while after the cmc it is mainly due to dilution of micelles. Thus, the micellisation enthalpy is calculated by Eq. (2):

$$\Delta_{mic}H^0 = -\Delta_{dem}H \quad (2)$$

The free energy and entropy of micellisation were calculated using a classical pseudophase separation model (Eqs. (3) and (4)),⁹ where α is the dissociation degree calculated by conductometric titrations (Table 1).²²

Cmc values obtained by ITC and conductometric titrations at different Gl^+ concentrations are given in Table 2. The observed differences are due to different physical properties probes.⁹

Table 1. Angular (B), linear (A), and correlation (R) coefficients obtained from linear fitting of conductometric titrations, before (label 1) and after (label 2) the cmc.

[GA]/mM	R ₁	A ₁	B ₁	R ₂	A ₂	B ₂	α^*
03	0.99615	0.3658	0.0690	0.99958	0.6357	0.0321	0.466
05	0.99999	0.5801	0.0501	0.99677	0.7150	0.0337	0.673
10	0.99976	1.0610	0.0572	0.99626	1.2152	0.0306	0.534
15	0.99974	1.5203	0.0504	0.99740	1.6354	0.0317	0.629

$$*\alpha = B_2/B_1$$

Table 2. Comparison of cmc values determined by ITC and conductometric titrations.

[Gl ⁺]/ (mM)	0	3	5	10	15
cmc _{ITC}	8.5	7.6	6.9	4.2	3.8
cmc _{Cond}	8.5	7.1	6.7	5.4	5.1

$$\Delta_{mic}G^0 = (2 - \alpha)RT \ln(\text{cmc}/[H_2O]) \quad (3)$$

$$T\Delta_{mic}S^0 = \Delta_{mic}H^0 - \Delta_{mic}G^0 \quad (4)$$

Micellisation of SDS is very well described in the literature as a process mainly driven by entropy. The key to understanding this entropy increase is the extensive hydrogen bonding that occurs in water. Because water forms no hydrogen bonds with the surfactant hydrophobic tail, the latter merely occupies a cavity in the liquid water structure and, as a result, water molecules become more ordered around the hydrocarbon with a decrease in entropy.⁷ On the formation of micelles, surfactant molecules are removed from water and form a micellar environment, which allows the cavity to revert to the structure of bulk water. The highly organised water structure involved in the cavity returns to normal hydrogen-bonded liquid water with an increase in entropy. Incidentally, enhanced hydrogen bonding at the walls of the cavity largely compensates for the breaking of hydrogen bonds to form the cavity. Thus, the low values of enthalpy are a balance between endothermic desolvation of monomers and exothermic electrostatic attraction between Na^+ cations and DS^- anions groups.^{7,9,23–25} Figures 3 and 4 show that cmc and $\Delta_{mic}G^0$ decrease as a function of the Gl^+ concentration, showing an increase in the spontaneity of the process.

Adding of electrolytes is known to affect the aggregation behaviour of surfactants. In the case of ionic surfactants, the influence of added electrolytes on their micellisation characteristics is attributed entirely to the counter-ion effect.²⁶ The general conclusions are that this stabilisation occurs through electrostatic interaction of the electrolytes with the surfactant ions in the Stern layer and with unbound counter-ions in the Gouy–Chapman diffuse double layer.⁹

Figures 5 and 6 show respectively enthalpy and entropy changes with Gl^+ concentration. In this work, the micellisation enthalpy at $[\text{Gl}^+] = 0$ was positive (0.84 kJ/mol)²⁵ In the presence of increasing concentrations of Gl^+ , reduction of enthalpy was observed, suggesting an increase in electrostatic interaction due to the preferential adsorption of Gl^+ in the surface of micelles. This hypothesis is corroborated by an increase in entropy, which is attributed to the desolvation of micelles upon Gl^+ adsorption.

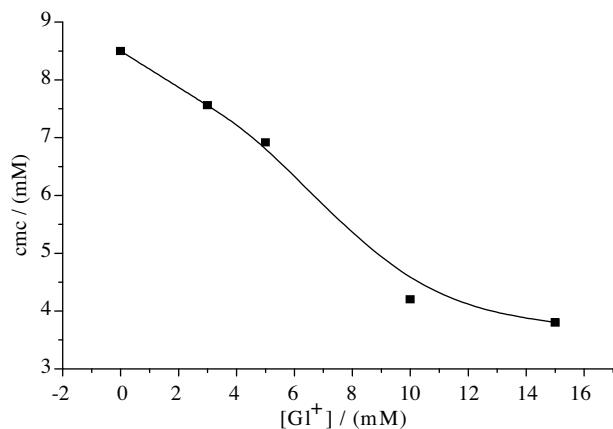


Figure 3. Plot of cmc against Gl^+ concentration, in water (pH 6.9) at 298.15 K.

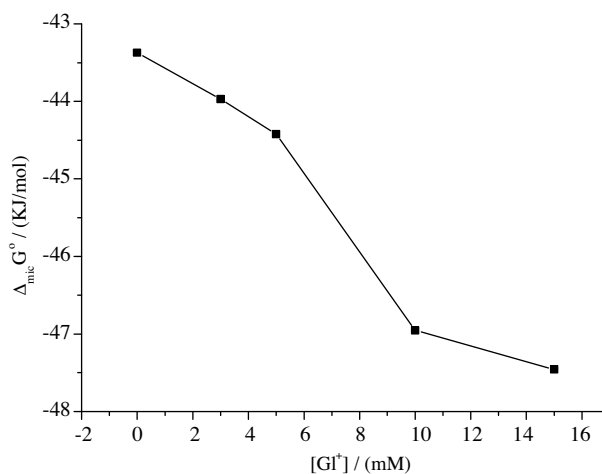


Figure 4. Plot of $\Delta_{mic}G^0$ against Gl^+ concentration, in water (pH 6.9) at 298.15 K.

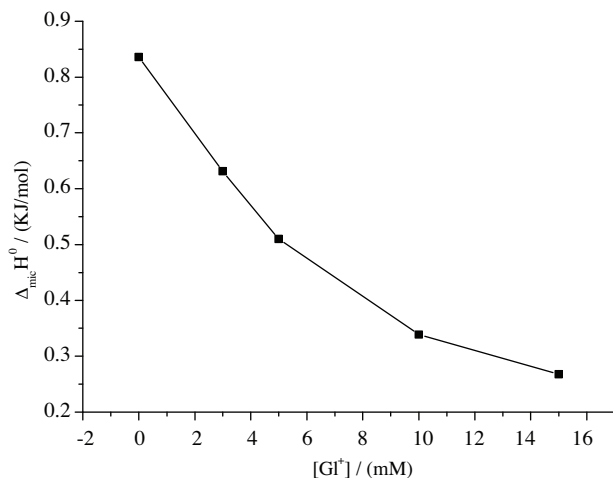


Figure 5. Plot of $\Delta_{mic}H^0$ against Gl^+ concentration, in water (pH 6.9) at 298.15 K.

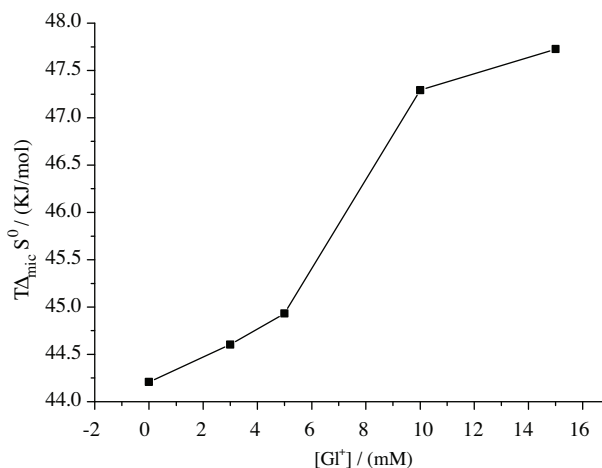


Figure 6. Plot of $T\Delta_{mic}S^0$ against Gl^+ concentration, in water (pH 6.9) at 298.15 K.

As described in the literature, large and polarisable ions, which tend to be less hydrated, bind more effectively to micelles.²³ Gl^+ is a bulky ion able to share the anionic charge of DS^- groups, favouring the micellisation more than small ions. Indeed, at cation concentration of 10 mM (Na^+ , Gl^+) and having Cl^- as counterion, $\text{cmc}_{\text{Gl}^+} = 4.20 \text{ mM} < \text{cmc}_{\text{Na}^+} = 5.8 \text{ mM}^{[*]}$ ([*] data not shown).

3.2. Gl^+ inducing SDS micellisation

In order to evaluate the Gl^+ /SDS interactions in a stepwise way, Gl^+ was titrated with SDS solution at constant concentration of 7.7 mM (around the cmc) and monitored by conductometric titrations, ITC, and ZP.

3.2.1. Conductometric titrations

Conductometric titrations were used in order to evaluate the electrostatic interactions in Gl^+ /SDS. Figure 7 shows the titration with Gl^+ 50.0 mM of 25.0 mL of SDS solution 7.7 mM, where can be observed at least 3 distinct ranges with different rates, separated by 2 concentrations named C_1 and C_2 .

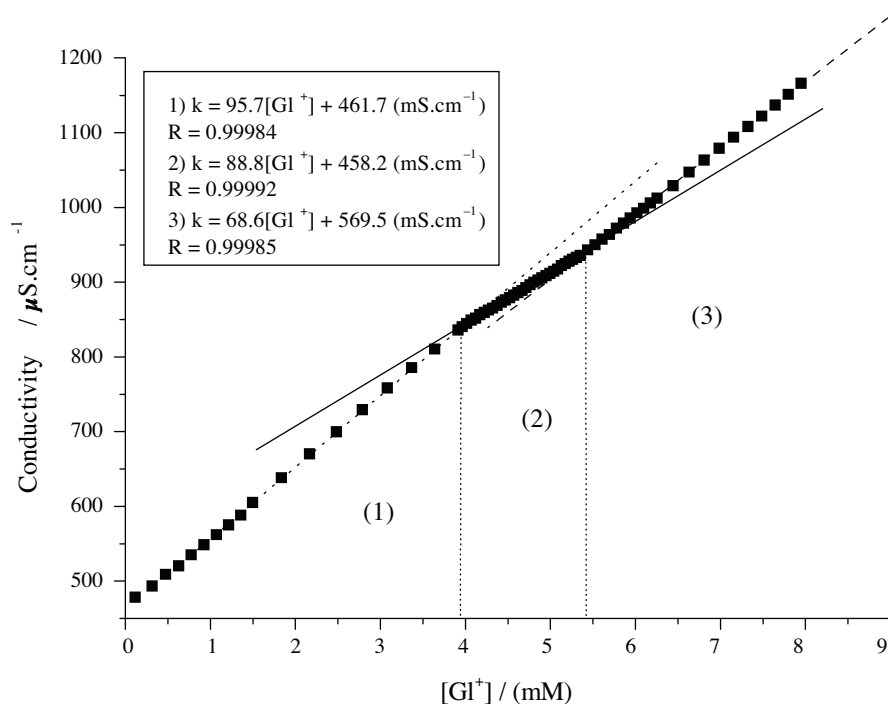


Figure 7. Conductometric titration of G1^+ 65.0 mM into cell charged with 25.0 mL of SDS 7.7 mM at 298 K.

The first range, between 0 and 4 mM, the rate assumes its greater value, $\partial k / \partial [\text{G1}^+] = 95.7 \mu\text{S.L/cm.mol}$. Considering that SDS micellisation is a quite cooperative phenomenon and that at this concentration a significant amount of micelles might exist, we attributed the behaviour in this range as micellisation induced by electrostatic interaction of G1^+ with SDS monomers. At G1^+ concentration $C_1 = 4$ mM we think that the micellisation process has finished.

At concentrations between $C_1 = 4$ and $C_2 = 5.4$ mM of G1^+ , micellar neutralisation by G1^+ is responsible for reducing the conductivity rate ($\partial k / \partial [\text{G1}^+] = 68.6 \text{ mS.L/cm.mol}$).

When the concentration of G1^+ reaches $C_2 \geq 5.4$ mM, the conductivity rate increases again ($\partial k / \partial [\text{G1}^+] = 88.8 \text{ mS.L/cm.mol}$). After this concentration, it is thought that the surface of the micelles is saturated and the concentration of free G1^+ cations increases again.

3.2.2. Isothermal titration calorimetry of G1^+ into SDS

Figure 8A shows the molar partial enthalpy of G1^+ versus the concentration of G1^+ ($\Delta_{G1}H \times [\text{G1}^+]$) at 298 K, in the presence of SDS solution at 7.7 mM (titration curve), with similar transitions observed to the conductivity experiments ($C_1 = 3.1$ mM and $C_2 = 6.9$ mM). Differences in C_1 and C_2 values are due to the probe used in each analytical technique.⁹ For comparison purposes, the dilution curve of G1^+ in water (blank experiment) is also presented.

According to the $\Delta_{G1}H^0$ data, the process is initially endothermic. During the titration, $\Delta_{G1}H^0$ becomes exothermic, suggesting competition among different phenomena. As mentioned in section 3.1, the micellisation process has been reported to be endothermic, occurring with increases in entropy^{7,9,25} Thus, the initial endothermic values of $\Delta_{G1}H^0$ can be the result of the G1^+ inducing micellisation, as discussed in the conductometric experiment. However, after the micellisation, the partial neutralisation of SDS micelles by G1^+

cations must be an exothermic process due to the electrostatic interactions. Above 6.9 mM, the Gl^+ dilution process predominates and $\Delta_{\text{Gl}}H^0$ is constant.

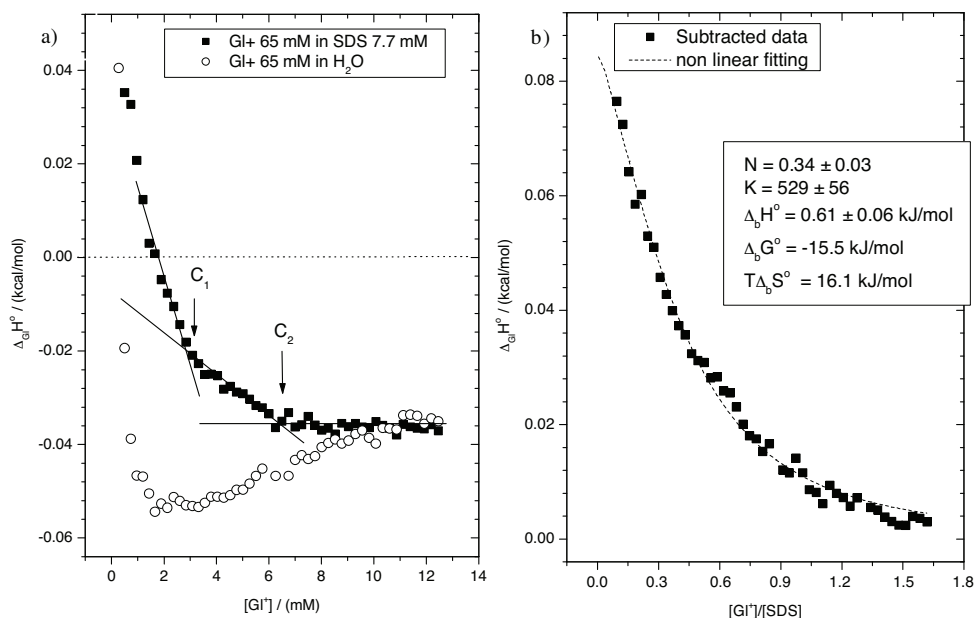


Figure 8. A) ITC data for titration of Gl^+ 65 mM into cell charged with 1.5 mL of SDS 7.7 mM, in water (pH 6.9) at 298.15 K. B) Data modelled by Wiseman isotherm after subtraction of the blank experiment.

In order to contribute to the discussion about the mechanism of Gl^+ /SDS interaction in comparison with other interacting systems, we modelled the titration curve by use of the Wiseman isotherm (Eq. (5)).²⁷ The analyses were performed in Microcal Origin 5.0 software (for ITC) after subtraction of the blank experiment^{27–29}

$$\left(\frac{dQ}{d[\text{Gl}^+]_{tot}} \right) = \Delta_b H^0 V_0 \left[\frac{1}{2} + \frac{1 - X_R - r}{2\sqrt{(1 + X_R - r)^2 - 4X_R}} \right] \quad (5)$$

Eq. (5) relates the stepwise change in the heat of the system normalised with respect to titrant concentration ($dQ/d[\text{Gl}^+]_t$) to the absolute ratio of ligand to receptor concentration ($X_R = [\text{Gl}^+]_t/[\text{SDS}]_t$). The parameters $\Delta_b H^0$, V_0 , and r are, respectively, the molar enthalpy of binding, the effective volume of the solution in the titration cell, and a composition variable $1/[\text{SDS}]_t \cdot K_b$, which is related to the equilibrium constant K_b for the binding process:



$$K_b = \frac{[\text{Gl}_x^+ : \text{DS}_y^-]}{[\text{Gl}^+]^x [\text{DS}^-]^y} \quad (7)$$

By using Eqs. (8) and (9), the free energy and entropy of binding were calculated.

$$\Delta_b G^0 = -RT \ln K_b \quad (8)$$

$$\Delta_b G^0 = \Delta_b H^0 - T\Delta_b S^0 \quad (9)$$

Figure 8B shows the titration curve after the subtraction of the blank experiment and the thermodynamic parameters. As can be observed, entropy ($T\Delta_b S^0 = +16.1$ kJ/mol) is the main contribution to the free energy of the binding process, which is attributed to the desolvation caused by electrostatic adsorption of Gl^+ on the micelles surface. This supposition is compatible with the positive value of enthalpy ($\Delta_b H^0 = +0.61$ kJ/mol), which is attributed to the breakdown of hydrogen and ion-dipole bonds during desolvation.

The binding constant obtained by this method was relatively low when compared to other highly specific systems ($K_b > 20,000$).^{28–31} However, the value of $K_b = 529$ is close to those found for drug binding in SDS micelles^{32,33} or in liposome systems.³⁴

Important information can also be obtained by analysis of stoichiometric coefficient N , which suggests a supramolecular structure formed by 0.34 Gl^+ for each DS^- molecule. Considering an average aggregation number of 62 surfactant molecules per micelle of SDS,³⁵ it was possible to estimate the amount of 21 Gl^+ molecules required to saturate a micellar solution. This value is similar to that of other SDS systems with small molecules, as described by Waters et al.³⁶

3.2.3. Zeta potential

The ZP reflects the electrostatic potential energy of the particles' surface, which is influenced by the changes in the interface with the dispersion medium. Thus it depends on the dissociation degree of the micelle and preferential adsorption of ions. The ZP measurements are presented in Figure 9, where addition of Gl^+ cations to aqueous solution of the SDS (7.7 mM) led to significant changes in ZP.

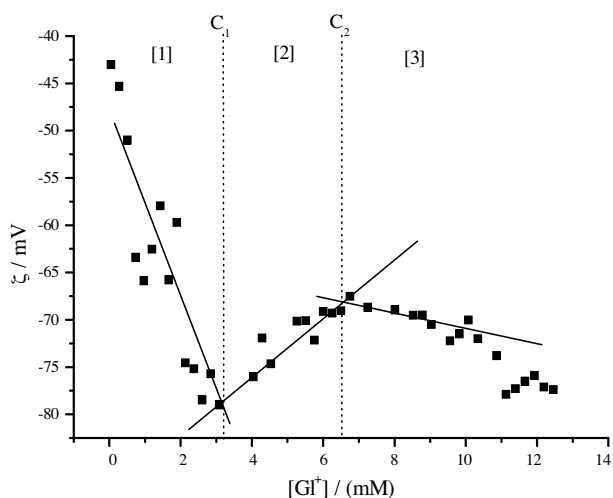


Figure 9. Zeta potential titration of Gl^+ 65.0 mM into cell charged with 25.0 mL of SDS 7.7 mM at 298 K. Measurements recorded in folded capillary cell (DTS1060) with 1.0 cm of optical length, Malvern Standard.

During the overall range of titration, the system showed negative values of ZP, which can be explained by the residual charge in anionic sulphate groups in the surface of the micelles, which are not entirely neutralised by Na^+ or Gl^+ . However, 3 ranges can also be identified, in a similar way to observed in conductometric titrations and ITC:

Range I: At the beginning, the SDS solution (7.7 mM) without Gl^+ presented a ZP value of -43 mV. The ZP values become more negative with the addition of Gl^+ , being attributed to micellisation induced by Gl^+ . New micelles contribute to the ZP becoming more negative.

Range II: In this range of the graph, the ZP becomes less negative, as a consequence of partial neutralisation of the micelles' surface.

Range III: After C_2 , ZP became more negative again. In this range it is expected to saturate the assemblies' surface, followed by an increase in GI^+ ions in the bulk of the solution. Thus, reduction in ZP could be explained by ionic exchange between GI^+ (large) and Na^+ (small), leading to a swelling of the outer layer.

3.3. NMR NOESY

In order to evaluate the spatial topology of the SDS/ GI^+ assembly, NOESY experiments of the SDS(15 mM)/ GI^+ (5 mM) system in D_2O at 25 °C were conducted.

Figure 10 shows the contour map of NOESY, where the cross peaks indicate the proximity between nuclei within the limit of 5 Å in the space, due to electromagnetic dipolar coupling.^{37–40} Cross peaks can be observed between SDS-H1 hydrogens and H6- and H11- GI^+ hydrogens, indicating that the protons are spatially close. These results agree with ITC and ZP results, where it was proposed that GI^+ cations interact with the SDS surface. It is important to stress that no cross peak was found between GI^+ hydrogens with H2-, H3-, or H4-SDS hydrogens, suggesting that there is no penetration of hydrophilic GI^+ into the core of micelles.

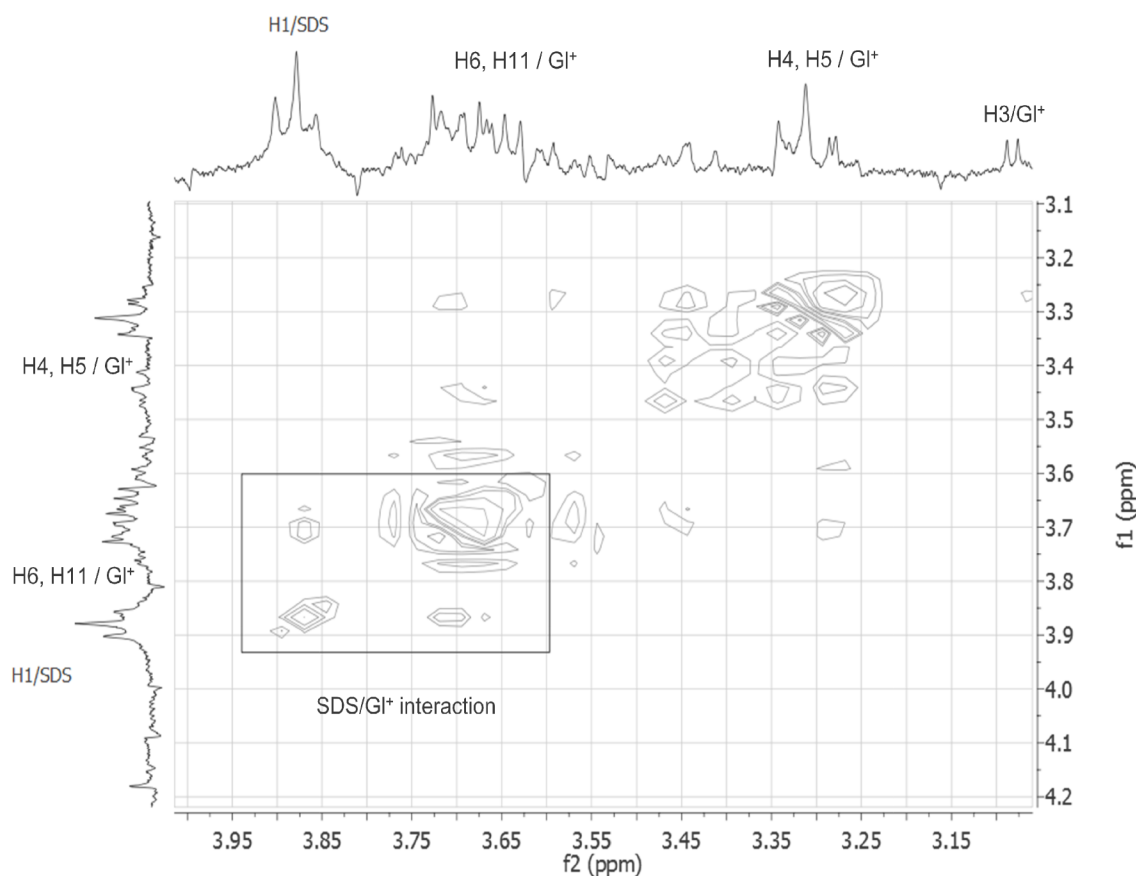


Figure 10. a) Expanded NOESY (300 MHz) contour map of SDS(15 mM)/ GI^+ (5 mM). F2 and F1 range from δH 3.0–4.0. Experiments were performed in D_2O at 298 K.

4. Conclusions

The supramolecular interactions between Gl^+ and SDS micelles have been described. Gl^+ reduces the cmc as a result of its ability to share charges in the micellar surface. Moreover, Gl^+ reduces the enthalpy and increases the entropy of micellisation due to the electrostatic attraction between Gl^+ and DS^- moieties, followed by high desolvation. By titration of SDS solution with Gl^+ , it was observed that at low concentrations, Gl^+ induces SDS micellisation. With the increase in Gl^+ concentration, neutralisation of the micellar surface is the predominant effect, followed by the Gl^+/Na^+ ionic exchange at high Gl^+ concentration. Considering the interaction as a binding process, the low equilibrium constant suggests nonspecific adsorption with an estimate of 20 Gl^+ molecules bound in the SDS micellar surface. Thus, it may be inferred that Gl^+ causes electrostatic disturbances in amphiphilic surfaces by different ways at different concentrations, before acting on the intramembrane environment. Possibly these phenomena change the permeability of the membrane for proteins and other biomolecules.

Acknowledgements

The authors are grateful to the Fundação de Amparo à Pesquisa do Estado de Minas Gerais (FAPEMIG: APQ-01243-10, APQ-00645-12) and Conselho Nacional de Desenvolvimento Científico e Tecnológico (CNPq: DT-310145/2011-2, MCT/CNPq-NANO: 550321/2012-8). This work is a collaborative research project with members of the Rede Mineira de Química (RMQ), who are supported by FAPEMIG.

References

1. Catuogno, C.; Jones, M. N. *Colloids Surface A*. **2000**, *163*, 165–176.
2. Cavalcanti, L. P.; Konovalov, O.; Torriani, I. L.; Haas, H. *Nucl. Instrum. Meth. B* **2005**, *238*, 290–293.
3. Duarte, A. M. S.; Wolfs, C. J. A. M.; Van Nuland, N. A. J.; Harrison, M. A.; Findlay, J. B. C.; van Mierlo, C. P. M.; Hemminga, M. A. *BBA-Biomembranes* **2007**, *1768*, 218–227.
4. Verly, R. M.; Rodrigues, M. A.; Daghashtanli, K. R.; Denadai, A. M.; Cuccovia, I. M.; Bloch, C., Jr.; Frezard, F.; Santoro, M. M.; Pilo-Veloso, D.; Bemquerer, M. P. *Peptides* **2008**, *29*, 15–24.
5. Carrozzino, J. M.; Khaledi, M. G. *J. Chromatogr. A*, **2005**, *1079*, 307–316.
6. Charaf, U. K.; Hart, G. L. *J. Soc. Cosmet. Chem.* **1991**, *42*, 71–85.
7. Frank, H. S.; Evans, M. W. *J. Soc. Cosmet. Chem.* **1945**, *13*, 507–532.
8. Loh, W.; Teixeira, L. A. C.; Lee, L. T. *J. Phys. Chem. B* **2004**, *108*, 3196–3201.
9. Evans, D. F.; Wennerstrom, H. *The Colloidal Domain: Where Physics, Chemistry, Biology, and Technology Meet*. 2nd ed, Wiley-VCH: New York, NY, USA, 1999.
10. Hsu, W. L.; Li, Y. C.; Chen, H. L.; Liou, W.; Jeng, U. S.; Lin, H. K.; Liu, W. L.; Hsu, C. S. *Langmuir* **2006**, *22*, 7521–7527.
11. Wang, G. S.; Pierens, G. K.; Treleaven, W. D.; Sparrow, J. T.; Cushley, R. J. *Biochemistry-US* **1996**, *35*, 10358–10366.
12. Moraes, L. G. M.; Fazio, M. A.; Vieira, R. F. F.; Nakaie, C. R.; Miranda, M. T. M.; Schreier, S.; Daffre, S.; Miranda, A. *BBA-Biomembranes* **2007**, *1768*, 52–58.
13. Raquel, K. B. B.; Bugs, M. R.; Neto, A. A.; Ward, R. J. *Biophys. Chem.* **2007**, *125*, 213–220.
14. Nielsen, A. D.; Arleth, L.; Westh, P. *BBA-Proteins Proteomics* **2005**, *1752*, 124–132.
15. Nielsen, A. D.; Arleth, L.; Westh, P. *Langmuir* **2005**, *21*, 4299–4307.

16. Herrero-Beaumont, G.; Rovati, L. C.; Castaneda, S.; Alvarez-Soria, M. A.; Largo, R., *Expert Opin. Pharmacother.* **2007**, *8*, 215–225.
17. Herrero-Beaumont, G.; Ivorra, J. A. R.; Trabado, M. D. C.; Blanco, F. J.; Benito, P.; Martin-Mola, E.; Paulino, J.; Marenco, J. L.; Porto, A.; Laffon, A.; et al. *Arthritis Rheum.* **2007**, *56*, 555–567.
18. Altman, R. D.; Abramson, S.; Bruyere, O.; Clegg, D.; Herrero-Beaumont, G.; Maheu, E.; Moskowitz, R.; Pavelka, K.; Reginster, J. Y. *Osteoarthritis Cartilage* **2006**, *14*, 963–966.
19. Altman, R.D.; Abadie, E.; Avouac, B.; Bouvenot, G.; Branco, J.; Bruyere, O.; Calvo, G.; Devogelaer, J.P.; Dreiser, R.L.; Herrero-Beaumont, G.; et al. *Osteoarthritis Cartilage* **2005**, *13*, 13–19.
20. Gouze, J. N.; Gouze, E.; Popp, M. P.; Bush, M. L.; Dacanay, E. A.; Kay, J. D.; Levings, P. P.; Patel, K. R.; Saran, J. P. S.; Watson, R. S.; et al. *Arthritis Res. Ther.* **2006**, *8*, R173–R187.
21. Bjordal, J. M.; Klovning, A.; Ljunggren, A. E.; Slordal, L. *Eur. J. Pain* **2007**, *11*, 125–138.
22. James, J.; Mandal, A. B. *Colloids Surface B* **2011**, *84*, 172–180.
23. Maiti, K.; Mitra, D.; Guha, S.; Moulik, S. P. *J. Mol. Liq.* **2009**, *146*, 44–51.
24. Singh, O. G.; Ismail, K. *J. Surfactants Deterg.* **2008**, *11*, 89–96.
25. Volpe, P. L. O.; Silva, E. A. *Thermochim. Acta* **1995**, *257*, 59–66.
26. Umlong, I. M.; Ismail, K. *Colloids Surface A* **2007**, *299*, 8–14. 27. Turnbull, W. B.; Daranas, A. H. *J. Am. Chem. Soc.* **2003**, *125*, 14859–14866.
27. Denadai, Â. M. L.; Oliveira, A. M. d.; Daniel, I. M. P.; Carneiro, L.A.; Ribeiro, K. C.; Beraldo, H. d. O.; Costa, K. J. R. d.; Cunha, V. C. d.; Segura, M. E. C.; et al. *Supramol. Chem.* **2012**, *24*, 204–212.
28. Denadai, Â. M. L.; Silva, J. G. D.; Guimarães, P. P. G.; Gomes, L. B. S.; Mangrich, A. S.; Rezende, E. I. P. d.; Daniel, I. M. P.; Beraldo, H. d. O.; Sinisterra, R. D. *Mat. Sci. Eng. C* **2013**, *33*, 3916–3922.
29. Barcelo, F.; Capo, D.; Portugal, J. *Nucleic Acids Res.* **2002**, *30*, 4567–4573.
30. Barcelo, F.; Ortiz-Lombardia, M.; Portugal, J. *Biochim. Biophys. Acta* **2001**, *1519*, 175–184.
31. Maity, A.; Ghosh, P.; Das, T.; Dash, J.; Purkayastha, P. *J. Colloid Interface Sci.* **2011**, *364*, 395–399.
32. McHedlov-Petrossyan, N. O.; Timiy, K.; Vodolazkaya, N. A. *J. Mol. Liq.* **2000**, *87*, 75–84.
33. Russell, A. L.; Williams, B. C.; Spuches, A.; Klapper, D.; Srouji, A. H.; Hicks, R. P. *Bioorg. Med. Chem.* **2012**, *20*, 1723–1739.
34. Mutelet, F.; Guermouche, M. H.; Rogalski, M. *Chromatographia* **2003**, *57*, 729–733.
35. Waters, L. J.; Hussain, T.; Parkes, G. M. B. *J. Chem. Thermodyn.* **2012**, *53*, 36–41.
36. De Alvarenga, E. S.; Lima, C. F.; Denadai, A. M. L. *Z. Naturforsch. A* **2004**, *59*, 291–294.
37. Denadai, A. M. L.; Santoro, M. M.; Teixeira, A. V.; Sinisterra, R. D. *Mat. Sci. Eng. C* **2010**, *30*, 417–422.
38. Lula, I.; De Sousa, F. B.; Denadai, A. M. L.; de Lima, G. F.; Duarte, H. A.; Guia, T. R. D.; Faljoni-Alario, A.; Santoro, M. M.; de Camargo, A. C. M.; dos Santos, R. A. S.; et al. *Mat. Sci. Eng. C* **2012**, *32*, 244–253.
39. Gjerde, M. I.; Nerdal, W.; Hoiland, H. *J. Colloid Interf. Sci.* **1996**, *183*, 285–288.